A&A, 707, A192 (2026)
https://doi.org/10.1051/0004-6361/202557591

Astronomy & Astrophysics

4U 1556–60 as a very faint neutron star X-ray binary at 700 pc with an undetected radio jet

E. C. Pattie[1,2,⋆], T. J. Maccarone[2], T. Russell[3], M. Bachetti[4], N. Degenaar[1], and T. Kupfer[5]

[1] Anton Pannekoek Institute for Astronomy, University of Amsterdam, Postbus 94249, 1090 GE Amsterdam, The Netherlands
[2] Department of Physics and Astronomy, Texas Tech University, Lubbock, TX 79409-1051, USA
[3] INAF, Istituto di Astrofisica Spaziale e Fisica Cosmica, Via U. La Malfa 153, I-90146 Palermo, Italy
[4] INAF Osservatorio Astronomicodi Cagliari, Viadella Scienza 5, 09047 Selargius (CA), Italy
[5] Hamburger Sternwarte, University of Hamburg, Gojenbergsweg 112, 21029 Hamburg, Germany

Received 7 October 2025 / Accepted 10 February 2026

ABSTRACT

Context. 4U 1556–60 is a low-mass X-ray binary that was discovered more than 50 years ago as a persistent X-ray source; however, very little was known about it. Recently, *Gaia* obtained a parallax for the optical counterpart that places 4U 1556–60 at a distance of only about 700 pc, making it one of the closest X-ray binaries known to date. This close distance drastically alters what was previously assumed about the source.
Aims. We revisit 4U 1556–60 in light of the newly determined distance of 700 pc, reinterpreting its literature and presenting new X-ray and radio observations to better understand various characteristics of the system.
Methods. We investigated the optical spectra and luminosity and the X-ray spectral and timing properties, and we performed the first targeted radio observation for the source in 45 years. These can be used to infer binary and accretion properties from independent methods.
Results. We conclude that a scenario in which 4U 1556–60 is a candidate ultracompact neutron star X-ray binary at a distance of ∼700 pc is able to explain the observed properties of the source. It resides at a persistent X-ray luminosity of $\sim 2 \times 10^{34}$ erg s^{-1}, an unusual value for a typical X-ray binary, but similar to several ultracompact systems. The ratio of the X-ray to optical luminosity is very high, also suggesting a physically small accretion disk. The radio jet is undetected with a very deep upper limit of 3×10^{25} erg s^{-1}, which is about 10^3 times fainter than the expected black hole jet correlation, strongly indicating a neutron star accretor. The X-ray spectrum is dominated by a power law, and the X-ray timing properties are also consistent with observations of other very low accretion rate X-ray binaries. No spin or orbital periodicity are found in the X-ray data. Future observations, especially to determine its orbital period, will further aid in understanding 4U 1556–60.

Key words. accretion, accretion disks – binaries: general – stars: jets – stars: neutron – X-rays: binaries

1. Introduction

X-ray binaries (XRBs) are systems in which a neutron star (NS) or black hole (BH) accretes material from a companion star (Done et al. 2007). XRBs are usually transient, spending a significant amount of time in a faint, low activity quiescence between shorter, bright outburst events, though a small fraction are persistently accreting in an active state as well. There are several factors that govern the general behavior of an individual XRB, for example, the mass and spectral type of the companion, the orbital period, and whether the accretor is a black hole or neutron star.

4U 1556–60 was discovered as an X-ray source in 1972 by the *Uhuru* mission (Giacconi et al. 1972) and was soon classified as an XRB with a low-mass donor star (LMXB) based on the identification of an optical counterpart (Charles et al. 1979). Further X-ray and optical studies were performed by Motch et al. (1989), with an optical spectrum showing strong helium and weak hydrogen lines. The source distance was unknown and was assumed to be at a Galactic Center distance of ∼8 kpc, resulting in an X-ray luminosity of $\sim 5 \times 10^{36}$ erg s^{-1}, which is a very typical X-ray luminosity for a persistently active LMXB (Avakyan et al. 2023). The X-ray spectral shape was similar to XRBs with neutron star accretors; however, the lack of thermonuclear Type I X-ray bursts in any of the X-ray data accumulated for 4U 1556–60 at an assumed luminosity of $\sim 10^{36}$ erg s^{-1} was problematic, though not strictly prohibitive, for a neutron star X-ray binary (NSXB) interpretation. There were also no X-ray pulsations detected, leaving the accretor nature undetermined. Later optical follow-up found strong Balmer lines in the optical spectrum and disfavored an ultracompact (i.e., a degenerate donor) interpretation for 4U 1556–60 (Nelemans et al. 2006).

Recently, *Gaia* Data Release 3 (Gaia Collaboration 2023) provided a parallax for the optical counterpart of 4U 1556–60 of 1.4530 ± 0.2644 mas, corresponding to a distance of 688^{+153}_{-106} pc. The median zero-point corrected geometric and photogeometric distances from Bailer-Jones et al. (2021) are 779 pc and 760 pc, respectively, and both are consistent with 700 pc within 1σ. This *Gaia* distance is an order of magnitude closer than previously assumed, which significantly changes many of the past interpretations of this source to date.

We reevaluate the properties of 4U 1556–60 based on a distance of ∼700 pc, present new X-ray and radio data, and propose that 4U 1556–60 is a very faint ultracompact NSXB with one of the weakest XRB radio jets observed to date. At a distance of

⋆ Corresponding author: e.c.pattie@uva.nl

about 700 pc it is also one of the closest X-ray binaries known to date and the closest low-mass Roche lobe overflowing XRB (Arnason et al. 2021).

2. Observations and data reduction

2.1. X-ray data: NICER

4U 1556–60 was observed with the Neutron Star Interior Composition ExploreR (NICER; Gendreau et al. 2016) for a total of 75 ks over the date range of 2023 Apr. 16 to 2023 May 04 (ObsIDs 658010101-658010110; a full list of observations are presented in Table 1). Data were processed in `HEASoft`[1] with `CALDB` version `20240206`. The data were reduced with the standard `nicerl2` pipeline calibration and filtering. The observations were analyzed individually as well as merged together with `niobsmerge`. Residual background flaring features persisted after calibration and these intervals were removed manually from the good time intervals with `xselect`. Spectra and light curves were then processed thorough `nicerl3-spect` and `nicerl3-lc` with `SCORPEON` background models, respectively[2].

2.2. Radio data: ATCA

4U 1556–60 was observed with the Australia Telescope Compact Array (ATCA; Wilson et al. 2011) on 2024 Nov. 09 to 2024 Nov. 10 in a single 12 hour observation resulting in 10.3 hours on-source (Table 2). The observation was recorded simultaneously in two frequency bands with 2 GHz bandwidth each, centered on 5.5 GHz and 9.0 GHz. The array was in its most extended 6A configuration with a maximum baseline of 6 km[3]. Flux density calibration was done using `PKS B1934-638`, and the phase calibrator was `B1613-586`. Data were processed using the Common Astronomy Software Applications (CASA; CASA Team 2022) using a standard calibration process. Each of the two separated frequency bands (4.5−6.5 GHz and 8−10 GHz) were calibrated independently, then the target data were imaged with the `tclean` task (`weighting=natural`), including phase self-calibration. The two self-calibrated frequency bands were then combined and imaged again with `tclean` and `gridder=mtmfs` to account for the large frequency span of the combined image.

3. Results

3.1. Distance of 700 pc

The *Gaia* parallax for the optical counterpart of 4U 1556–60 corresponds to a 1/parallax distance of about 700 pc. We first consider the scenario that this optical source is not the true counterpart and is rather an unrelated or interloper star. However, there are clearly broad optical emission lines in the spectrum of this counterpart that are attributed to accretion disks and not stellar emission, as well as a very blue continuum and an ultraviolet excess compared to a normal stellar spectral energy distribution (Charles et al. 1979). These features ensure that the emission of the optical counterpart source is indeed dominated by an accretion disk, strongly indicating its association with 4U 1556–60 as an XRB, rather than being an unrelated superimposed star dominating the optical emission. Additionally, 4U 1556–60 is located in a relatively low sky density region of the Galaxy ($l = +324°$, $b = -6°$), where there is an average of 0.03 *Gaia* sources per square arcsecond in the vicinity of 4U 1556–60. Thus the chance of an unresolved superposition of the *Gaia* counterpart (<0.4″ separation) based on the local stellar sky density is also low at 2.3%.

We next consider that there may be a fainter interloper star that could affect the observed parallax shift, such that there is a superimposed interloper star that is much closer than 700 pc while 4U 1556–60 is at a distance greater than 700 pc. This has indeed been observed to be the case for a different XRB, BW Cir (Gandhi et al. 2019). However, the proper motion measurements from *Gaia* Data Releases 2 and 3 for 4U 1556–60 are consistent with each other within 1σ, unlike BW Cir which showed a 2σ change in its proper motion between the two epochs as an artifact of the superposition evolving over time.

A further restriction on a potential interloper star is the faintness of the optical and infrared counterparts of 4U 1556–60, and especially the latter. A very faint infrared counterpart was detected by the Vista Hemisphere Survey (VHS; McMahon et al. 2013), located 0.2″ away from the *Gaia* position at a J band magnitude of 18.4. Following the absolute J band magnitudes for M and L dwarf stars in Hawley et al. (2002), if an interloper star is located at, for example, 200 pc it must be fainter than an L0 dwarf to not be brighter than the VHS counterpart. Then, using the inferred space density of L dwarfs from Cruz et al. (2007), we estimate that the *Gaia* superposition chance for L dwarfs out to 200 pc is $\sim 10^{-5}$, thus it is extremely unlikely that there is an interloping faint nearby dwarf star.

A final consideration is that there may be an unknown cold white dwarf interloper in *Gaia*, which may interfere with the optical parallax but would not distort the infrared spectral energy distribution of 4U 1556–60's counterpart (unlike a dwarf star above, which would be relatively bright in the infrared). *Gaia* Data Release 3 has been examined for white dwarf stars by Gentile Fusillo et al. (2021), who find that the sky density near the Galactic Plane of white dwarfs with G magnitudes ≤20 is about 6 per square degree. Thus, the chance that there is a superimposed white dwarf is again extremely unlikely at $\sim 10^{-6}$.

Therefore, we argue that the optical source observed by *Gaia* is indeed a singular and true counterpart to 4U 1556–60, providing a new distance of ∼700 pc, with an optical G magnitude of 19 and an amplitude of variability of about half of

Table 1. NICER X-ray observations of 4U 1556–60.

ObsID	Date (YYYY MM DD)	Exposure (ks)
658010101	2023 04 16	1.4
658010102	2023 04 17	15.7
658010103	2023 04 18	14.2
658010104	2023 04 19	13.6
658010105	2023 04 20	1.4
658010106	2023 04 21	7.3
658010107	2023 04 22	9.0
658010108	2023 04 23	4.7
658010109	2023 04 27	6.3
658010110	2023 05 04	1.2
Total		74.9

[1] Nasa High Energy Astrophysics Science Archive Research Center (Heasarc) 2014.
[2] NICER data analysis threads containing `nicerl3` and `SCORPEON`: https://heasarc.gsfc.nasa.gov/docs/nicer/analysis_threads/
[3] https://www.narrabri.atnf.csiro.au/operations/array_configurations/configurations.html

Table 2. ATCA radio observation of 4U 1556–60.

ObsID	Date (YYYY MM DD)	Obs. time	Freq. (GHz)	Upper limit (3σ, μJy)
C3652	2024 11 09 – 2024 11 10	12 h	5.5	13.8
			9.0	17.3
			7.25 (combined)	10.4

Notes. Single multifrequency ATCA radio observation and nondetection results of 4U 1556–60.

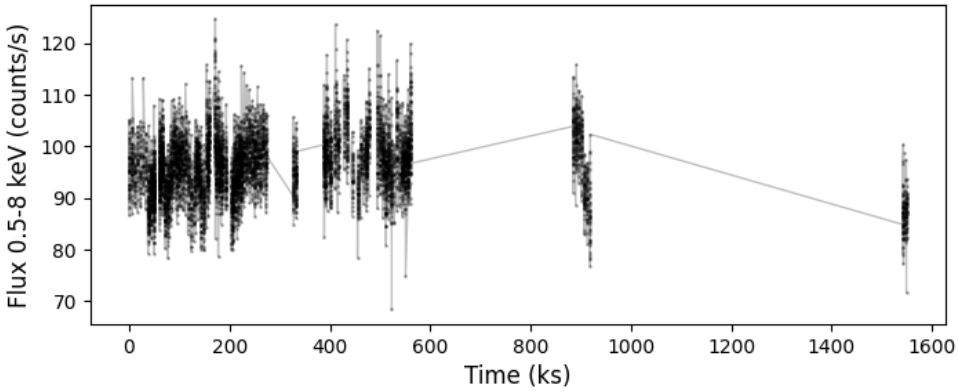

Fig. 1. NICER light curve of 4U 1556–60 from 0.5–8 keV with 8 s cadence after excluding residual background flaring features. Flux errors are not plotted and are typically about 5%. The stability of the flux observed in our NICER data justifies combining all observations to analyze spectral and timing properties. The light curve begins at MJD 60050.80902778.

a magnitude (Motch et al. 1985). The distance estimates from Bailer-Jones et al. (2021), the geometric value of 779^{+210}_{-153} pc and the photogeometric value of 760^{+198}_{-119} pc with 1σ uncertainties, are consistent with a distance of 650–950 pc. We subsequently use 700 pc moving forward, as a slightly smaller or larger distance does not significantly change our conclusions for 4U 1556–60.

3.2. X-ray data

Our recent NICER data are the first targeted X-ray observations of 4U 1556–60 in about 15 years. With these data, we investigated the spectral components and the presence of an iron line, and searched for evidence of pulse and orbital periods. The X-ray flux over the 75 ks of data is very stable (91% of light curve data are within 10% of the median; Fig. 1), therefore we combine all data for spectral analysis.

3.2.1. NICER timing

The NICER data were searched for an orbital and pulse period in the energy range of 0.5–8 keV. An orbital period was searched for by combining all NICER observations and extracting a 1 s light curve with `nicerl3-lc`. A Lomb-Scargle periodogram (via `astropy`; Astropy Collaboration 2013, `normalization='standard'`) was performed on both the NICER light curve and its window function to check for sampling biases. The resulting periodograms are shown in Fig. 2, with no statistical power at any frequency independent of the sampling biases indicated by the window function, thus there is no indication of an orbital period from the X-ray data. The sampling biases are consistent with the International Space Station's orbit of 93 minutes, and harmonics of this value. The NICER data are sensitive to ∼2% sinusoidal modulations in the light curve, except near sampling-biased frequencies where the sensitivity worsens up to ∼5%, for periods of up to ∼1 day. We also note that there were no Type I X-ray bursts detected in the light curve, a continuing feature of this source from past X-ray data.

A pulse period was searched up to 1500 Hz in the combined 75 ks of NICER data using `stingray` (Huppenkothen et al. 2019) to construct the power spectral density (PSD) from the barycenter-corrected event file. There are no discernible features in the PSD, notably lacking a candidate spin period with a fractional pulse amplitude $5 \times$ RMS upper limit of 1.06%. The individual observations also displayed identically featureless PSDs. We did not perform an acceleration search, as a pulse period in an ultracompact system with a very low-mass donor would result in a relatively small smearing effect, and no candidate pulse period was identified. Potential orbital acceleration smearing of the pulse period for a very low-mass donor star (discussed further later) is small ($\lesssim$0.3 Hz for a 500 Hz pulsar, which would have been resolved), thus we are very sensitive to a potential spin period without an acceleration search.

3.2.2. NICER spectrum

The spectrum of the combined 75 ks of 4U 1556–60 (Fig. 3) (`xspec` version `12.14.0h`; Arnaud 1996) is consistent with a nonthermal-dominated hard spectral state, with a flux of $\sim 3 \times 10^{-10}$ erg s^{-1} cm^{-2}, corresponding to a 2–10 keV luminosity of $\sim 2 \times 10^{34}$ erg s^{-1} at a distance of 700 pc. The spectrum is fit with a `powerlaw` + `bbodyrad`, and a `gaussian` for the iron line with an equivalent width of ∼8 eV (χ^2/d.o.f. = 41.37/115). Abundances and photoelectric cross sections for `phabs` are from `angr` (Anders & Grevesse 1989) and `vern` (Verner et al. 1996), respectively. Full fit parameters are in Table 3. The data were also similarly fit well statistically with a `diskbb` instead of a `bbodyrad` (χ^2/d.o.f. = 37.90/115); however, the normalization for `diskbb` in this case resulted in an apparent inner disk radius of <1 km at 700 pc, therefore we deemed `diskbb` unphysical and instead favor the `powerlaw` + `bbodyrad` to fit the continuum. The `bbodyrad` with a temperature of ∼0.9 keV has a characteristic radius of 0.21 ± 0.02 km from its normalization parameter.

We tested additional model scenarios for the spectrum. Fixing the `bbodyrad` component to a larger radius of 5 km resulted in a poor fit with χ^2/d.o.f. = 559.61/115 with strongly struc-

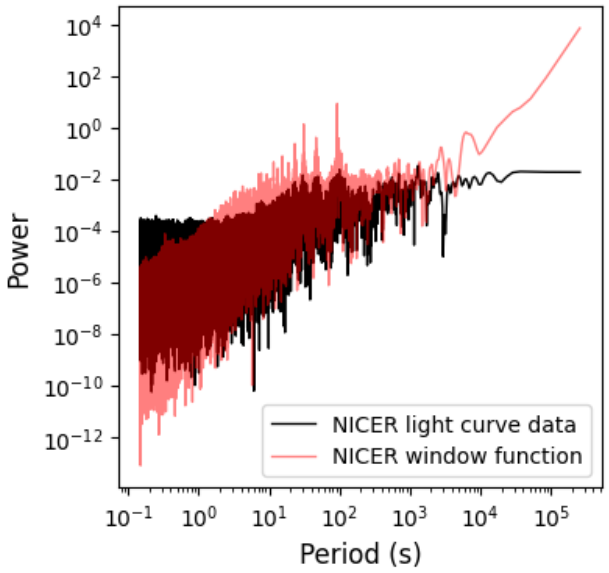

Fig. 2. Lomb-Scargle of the full 75 ks of NICER data with a light curve time resolution of 1 s. There are no statistical features of the Lomb-Scargle periodogram that are not biased by the light curve sampling, as shown by the NICER window function Lomb-Scargle for comparison. Thus, the NICER data also do not show a sign of an orbital period.

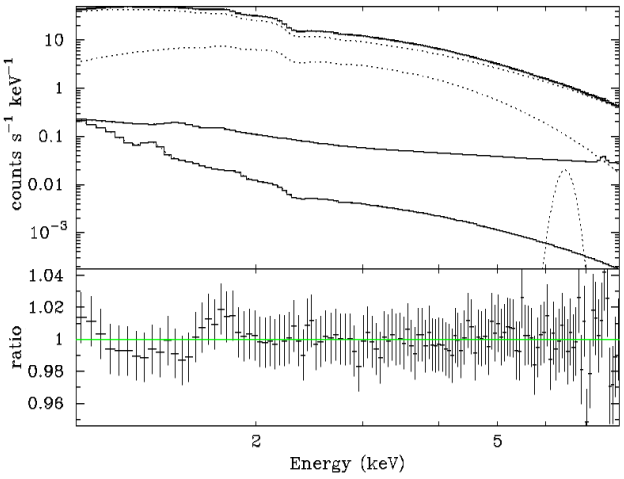

Fig. 3. X-ray spectrum of 4U 1556–60 from NICER from all observations combined. The spectrum is fit with a `powerlaw` + `bbodyrad`, and a `gaussian` for the iron line. Background models are also shown. Full parameters are in Table 3.

tured residuals. Removing the blackbody component and fitting the continuum with only a `powerlaw` resulted in a similarly poor fit with χ^2/d.o.f. = 618.12/116, again with strongly structured residuals. An attempt to use the `nsatmos` model (Heinke et al. 2006) instead of `bbodyrad` resulted in a failure to fit the spectrum due to the constrained range of the temperature parameter. A `comptt`-only model (Titarchuk 1994) was also poorly fit with χ^2/d.o.f. = 305/117. The spectrum was fit equally well with `comptt` + `bbodyrad` with χ^2/d.o.f. = 50.54/115 and blackbody parameters consistent with the `powerlaw` + `bbodyrad` of a hot and small (1.05 keV, 5.6 normalization) thermal component. Thus, the spectral fit necessitates a physically very small and hot thermal component in addition to a dominating nonthermal component.

Table 3. NICER X-ray spectral fit of 4U 1556–60.

Model	Parameter	Value
phabs	nH ($\times 10^{22}$)	$0.34^{+0.016}_{-0.015}$
bbodyrad	kT (keV)	$0.92^{+0.03}_{-0.04}$
	norm	$9.12^{+1.75}_{-1.56}$
	L_X (erg s^{-1})	*~4 × 10^{33}*
	radius (km)	*0.21 ± 0.02*
powerlaw	PhoIndex	$1.53^{+0.04}_{-0.04}$
	norm	$5.66^{+0.4}_{-0.4} \times 10^{-2}$
gaussian	LineE (keV)	$6.46^{+0.14}_{-0.17}$
	Sigma (keV)	$0.16^{+0.17}_{-0.16}$
	norm	$2.83^{+0.002}_{-0.002} \times 10^{-5}$
	EqW (eV)	*7.83*
Chi-squared/d.o.f.	41.37/115	
Flux (2–10 keV)	(erg s^{-1} cm^{-2})	3.46×10^{-10}
L_X (2–10 keV)	(erg s^{-1})	1.97×10^{34}

Notes. Luminosities assume a distance of 700 pc. Data were fit in `xspec`.

3.2.3. Other X-ray data

4U 1556–60 is monitored by the Monitor of All Sky X-ray Image (MAXI; Matsuoka et al. 2009) telescope (source name 1H 1556–605), and over the last ~15 years its X-ray light curve has not shown any significant long-term variability, reinforcing the view that 4U 1556–60 persistently accretes at a very stable rate, corresponding to a median 2–8 keV luminosity value of 3×10^{34} erg s^{-1}. Other targeted X-ray data in the literature over the decades have also found similar fluxes and spectral shapes of a power law + thermal component (Motch et al. 1989; Farinelli et al. 2003a). There have been no outbursts or Type I bursts detected for 4U 1556–60.

3.3. Radio data

The ATCA radio data did not detect a radio counterpart to 4U 1556–60 with a 3σ upper limit of 10.4 μJy at 7.25 GHz (Fig. 4), corresponding to an upper limit for the radio luminosity of $\sim 3 \times 10^{25}$ erg s^{-1} at 5 GHz assuming a flat spectral index, as expected for LMXBs in their hard states (Fender 2001). This result and other XRB X-ray and radio luminosities are shown in Fig. 5.

4. Discussion

4.1. A neutron star accretor

It was generally believed that the accretor in 4U 1556–60 was a neutron star, primarily based on its X-ray spectral properties. Our recent radio data, an upper limit of 3×10^{25} erg s^{-1} and the first targeted observation since Duldig et al. (1979) (<5 mJy nondetection), provide the strongest evidence that the accretor in 4U 1556–60 is indeed a neutron star. The correlation between radio and X-ray luminosity (Fender et al. 2004; Gallo et al. 2018), L_R–L_X, shown in Fig. 5, can be used as a diagnostic of the nature of the accretor for unambiguous cases due to the ubiquitous presence of black hole X-ray binary (BHXB) jets in hard spectral states, including detections in quiescence for some brighter systems (e.g., Gallo et al. 2006; Corbel et al. 2008; Soleri & Fender 2011). The upper limit we

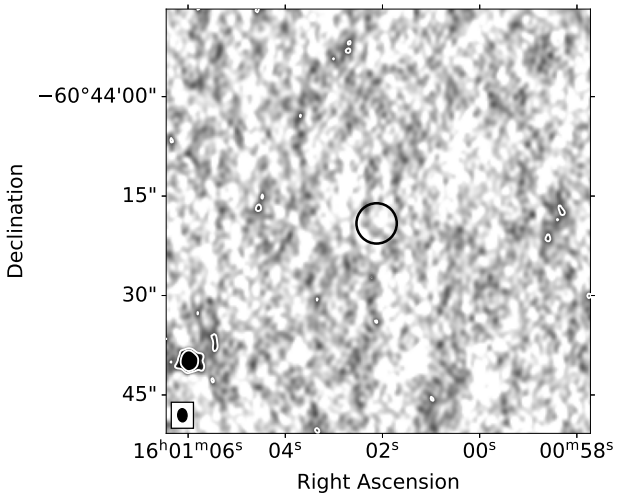

Fig. 4. ATCA radio image of 4U 1556–60 at the combined frequency of 7.25 GHz. The black circle is centered on the *Gaia* optical counterpart for visual reference. The contours plotted are 3σ and 10σ, where σ is the background RMS value of 3.5 μJy. The bright source in the lower left corner has a peak flux density of 174 μJy ($\sim 50\sigma$).

obtained shows that 4U 1556–60 has a radio jet that is at least three orders of magnitude fainter than the BHXB population at a similar X-ray luminosity. Thus, this upper limit on the radio jet luminosity indicates that 4U 1556–60 almost certainly hosts a neutron star that is producing a much weaker jet relative to the expectation of BHXBs at similar X-ray luminosities. We return to further implications of 4U 1556–60's radio jet luminosity later in the discussion in Section 4.4.

It is again noteworthy that 4U 1556–60 has never shown Type I bursts, which are a very common though not universal feature of accreting neutron stars with low magnetic field strengths typical of NS LMXBs (Lewin et al. 1993; Degenaar et al. 2018; Galloway et al. 2020). We can calculate the expected burst rate for hydrogen bursts using $\alpha = L_{\rm pers} \times t_{\rm rec}/E_{\rm burst}$, where α is a value between 40–100 (Strohmayer & Bildsten 2006), $L_{\rm pers}$ is the persistent X-ray luminosity, $t_{\rm rec}$ is the burst recurrence time, and $E_{\rm burst}$ is the fluence of the burst. We estimate that the recurrence time of standard hydrogen bursts for 4U 1556–60 is $\gtrsim 10^3$ ks, or about 10 bursts per year, assuming typical LMXB accretion disk abundances dominated by hydrogen. With this inferred burst rate, the lack of bursts detected in the accumulated but sporadic X-ray data of 4U 1556–60 to date is indeed expected.

This is still a conservative under-estimation of the recurrence time due to the very low X-ray luminosity of 4U 1556–60, as the neutron star itself will be much cooler than more typical, higher persistent X-ray luminosities thus requiring a more massive buildup of material before ignition (Peng et al. 2007). This may result instead in even more infrequent "intermediate" duration bursts which have been observed in other NSXBs at similarly low X-ray luminosities (e.g., Degenaar et al. 2010; Alizai et al. 2023). Thus, 4U 1556–60 may be slowly building up a very thick layer of hydrogen or helium, enabled by the low accretion rate delaying the fuel reaching the critical ignition temperature, and possibly steadily fusing hydrogen into helium as well. It would then very rarely exhibit a luminous intermediate duration burst with recurrence times possibly as long as several years or more (Kuulkers et al. 2009; Alizai et al. 2023). If 4U 1556–60 does burst, then it may be a nearby analog or member of the "burst-only" NSXBs usually observed at Galactic Center distances where low luminosity persistent X-ray emission is often not detected (e.g., Cocchi et al. 2001; Cornelisse et al. 2002).

There are no reported *Swift* Burst Alert Telescope (BAT; Barthelmy et al. 2005) triggers in the direction of 4U 1556–60 (none within 1°), and similarly there is no over-density of *Fermi* Gamma-Ray Burst Monitor (GBM; Meegan et al. 2009) triggers. At 700 pc, BAT and GBM are able to detect Type I bursts as they have for other NSXBs at greater distances (Linares et al. 2012; Jenke et al. 2018; in't Zand et al. 2019; Lin & Yu 2020). Thus, BAT and GBM both provide additional indications that the burst rate of 4U 1556–60 is extremely low, of order $\lesssim$1 burst/year.

Another potential is that 4U 1556–60 hosts a very strong magnetic field of $\gtrsim 10^{12}$ G, which observationally inhibits the ability of NSXBs to burst. This is believed to be due to magnetic confinement of the accreting material driving persistent burning (Joss & Li 1980). This possibility will be discussed further below in Section 4.3.

4.2. Ultracompact nature and binary parameters

Ultracompact X-ray binaries (UCXBs) are a class of XRBs that have short orbital periods of $\lesssim$80 minutes (Savonije et al. 1986; van Haaften et al. 2012). Main sequence donor stars cannot fit within their Roche lobe at these orbital periods, thus UCXB donors are necessarily degenerate white dwarfs or semi-degenerate helium stars. UCXBs are of particular interest, for example, as products of common envelope evolution (Paczynski 1976; Ivanova et al. 2008), as progenitors of radio millisecond pulsars (Tauris et al. 2012), and as gravitational wave sources (Nelemans et al. 2001; Chen et al. 2020). They are hydrogen-poor and thus some other their behaviors may be affected, such as bursts in NS UCXBs. There are about 50 known or candidate UCXBs to date (Armas Padilla et al. 2023), with 20 of them confirmed via orbital period measurements. Their population disproportionally resides in globular clusters likely due to the much higher rate of dynamical interactions between stars there (Verbunt 1987; Ivanova et al. 2008).

We present multiple methods to estimate or explain the orbital period in 4U 1556–60. Although none of these individually are robust enough to determine the orbital period definitively, altogether these suggest that the orbital period is likely to be ultracompact.

4.2.1. Optical and infrared luminosity

The optical magnitude of the *Gaia* counterpart is about 19, with a distance modulus of 9.2 magnitudes and an additional 1 magnitude to account for extinction based on the NASA/IPAC Extragalactic Database calculator[4]. Thus, we estimate that the absolute optical magnitude of 4U 1556–60 is about 8.8 magnitudes. The VHS infrared J band counterpart is about 18.4 magnitudes, thus an absolute magnitude of 9.4.

In XRBs, the observed optical and infrared (OIR) emission is a combination of the donor star's light and reprocessed X-ray emission from the accretion disk, and possibly jet emission. In LMXBs, the disk reprocessing dominates the optical emission when the source is not in quiescence

[4] https://ned.ipac.caltech.edu/extinction_calculator

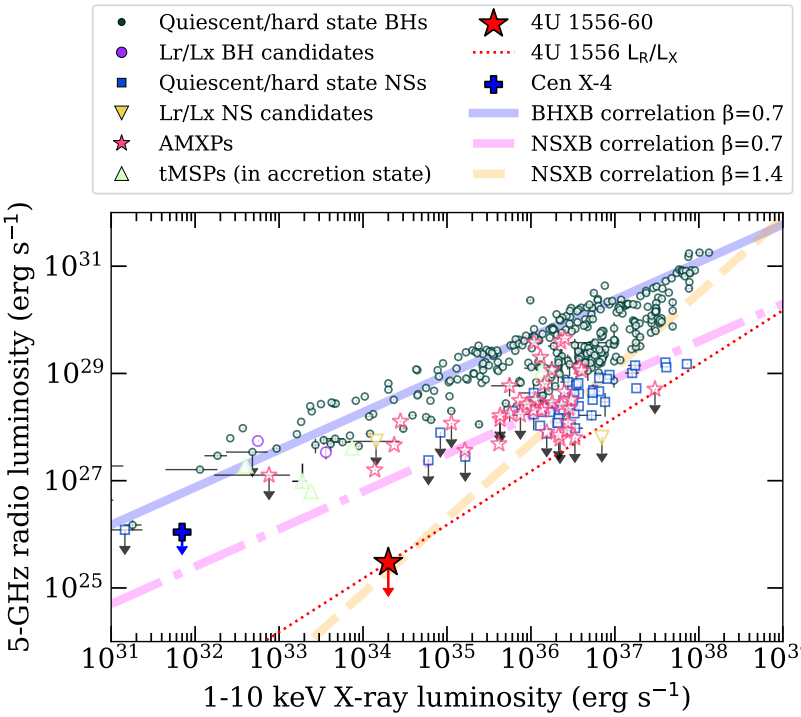

Fig. 5. Plot of X-ray binary radio and X-ray luminosities from Bahramian & Rushton (2022), with our radio nondetection of 4U 1556–60 indicated with a red star and a line of constant L_R/L_X plotted for reference at other source distances. Three correlation lines are plotted for visual reference: solid blue for BHXBs; dash-dot magenta for NSXBs with $\beta = 0.7$; and dashed orange for NSXBs with $\beta = 1.4$. AMXPs are accreting millisecond pulsars with stronger magnetic fields than general NSXBs, and tMSPs are transitional millisecond pulsars whose radio emission during their XRB-like state is thought to not arise from a jet alone. The very low upper limit of 4U 1556–60's radio emission for its X-ray luminosity is strongly indicative of a neutron star accretor, as it is about 1000 times fainter than expected for a black hole accretor. The previous deepest upper limit in radio luminosity for a NSXB, Cen X–4 in quiescence at ∼1.2 kpc (van den Eijnden et al. 2022), is also shown as a blue plus sign.

(van Paradijs & McClintock 1994; hereafter vPM94). The optical spectra of 4U 1556–60 did not show any stellar features (Motch et al. 1989; Nelemans et al. 2006), thus we can assume that the optical emission is similarly dominated by the accretion disk rather than by the donor star. We do not consider OIR jet emission due to the radio nondetection.

Simple test cases for the orbital period can be performed given the requirement that 4U 1556–60 must have a Roche lobe filling donor star in an orbit with an assumed 1.4 $M_\odot$ neutron star. If 10% of the optical light is emitted from the companion (and the rest from the disk reprocessing X-ray emission), a donor star with an absolute visible magnitude of 11.3 corresponds to a type M3, and thus an orbital period of about 3 hours. If only 1% of the optical light is from the companion, then the 13.8 magnitude M5 donor star would have an orbital period of 2 hours.

Similarly using the VHS counterpart, a star with an absolute J band magnitude of 9.4 would correspond to an early L dwarf. Assuming this L dwarf produces all of the observed infrared counterpart's emission, the orbital period would be only 2 hours, and again this is an over-estimation of the donor emission contribution and thus orbital period. Therefore, the faintness of the OIR counterpart alone places strong upper limits on the orbital period of 4U 1556–60 due to the requirement that the donor star fill its Roche lobe in this system.

4.2.2. X-ray:OIR ratio

The X-ray luminosity can also be utilized in combination with OIR to estimate the size of the accretion disk, and therefore estimate the orbital period of the binary. A very high X-ray to optical luminosity ratio indicates that there is a physically small accretion disk surface area which is reprocessing the X-ray emission. vPM94 utilizes this to roughly estimate the orbital period of LMXBs based on their X-ray luminosity and absolute optical magnitude during times of active accretion when the donor star emission is a negligible contribution to the total optical light.

Following this for 4U 1556–60 with $L/L_{\rm Edd} \approx 10^{-4}$ and M_V of 8.8, the orbital period is estimated to be 60^{+110}_{-60} s. Though an orbital period of 60 s is certainly unphysical, the error of this is also quite large which we find is due to the quoted uncertainties of the best fit slope equation in vPM94, combined with the overall low X-ray and optical luminosities for 4U 1556–60. There is also significant scatter in the original relationship derived by vPM94 of about 0.5 in log Σ, which can increase the inferred period to be 6^{+10}_{-6} minutes at +0.5 log Σ, or 30^{+54}_{-30} minutes at +1 log Σ.

These results are plotted in Fig. 6, including the original data as well as a sample of UCXBs from Armas Padilla et al. (2023) which have X-ray and optical fluxes and known orbital periods. There is indeed scatter in the relation, in part from inclination angle effects, varying mass ratios, as well as non-simultaneity of the multiwavelength data. Overall, we believe this to broadly indicate that 4U 1556–60 indeed has a very short orbital period as evidenced by its faint optical counterpart, even if the above relation is not as precise at low X-ray and optical luminosities.

Similar to vPM94, Russell et al. (2006) investigated the correlation between X-ray and OIR emission of XRBs, considering both disk and jet contributions to the OIR emission and fitting BH and NS XRBs separately. Assuming that there is negligible OIR jet emission in 4U 1556–60 due to the radio nondetection, the *Gaia* counterpart again corresponds nominally to an unreasonably short orbital period of ∼4 minutes for a NSXB, but considering the scatter around this relation the inferred orbital period can reasonably be extended to 40 minutes. Using the VHS counterpart at 2.14 μm instead returned similar results with a nominally very short orbital period.

4.2.3. Unusual persistent X-ray luminosity

The X-ray luminosity of 4U 1556–60, stable since its discovery (e.g., Wood et al. 1984; Motch et al. 1989; Farinelli et al. 2003b, and since 2009 from MAXI), is at an unusual value of about

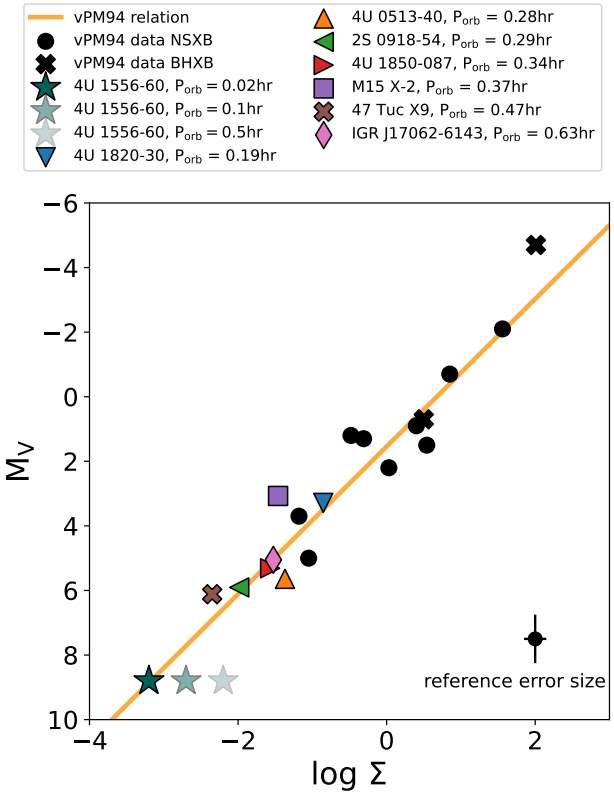

Fig. 6. Reproduced plot relating the absolute visual magnitude of LMXBs with the parameter $\Sigma = (L_X/L_{Edd})^{1/2}(P/1\,h)^{2/3}$ from van Paradijs & McClintock (1994). vPM94 NSXBs are black circles and BHXBs are black X's, with reference errors on a point in the lower right. We have added the nominal vPM94 relation line in orange. We have also added a sample of known UCXBs from Armas Padilla et al. (2023) in various colors and marker shapes. Estimations for the orbital period of 4U 1556–60 are shown in three blue stars with decreasing opacity, at +0, +0.5, and +1 log Σ respectively.

10^{34} erg s^{-1}. It is significantly brighter than typical quiescent XRBs (~10^{32} erg s^{-1}, e.g., Heinke et al. 2003; Wijnands et al. 2017), while also being much fainter than the majority of other persistently active systems (≳10^{36} erg s^{-1}, e.g., in't Zand et al. 2007). However, UCXBs are able keep their small accretion disks ionized at low X-ray luminosities via irradiation from the inner regions (van Paradijs 1996; Dubus et al. 1999), thus allowing them to be persistently active at lower X-ray luminosities than the more common longer period systems (Lasota 2001).

This persistent luminosity may also be related to a high mass transfer rate from the donor star. Transient XRBs have lower mass accretion than transfer rates in quiescence, thus causing the accretion disk mass to build up and trigger an instability. The subsequent outburst accretion rate exceeds the mass transfer rate and depletes the disk, ending the outburst (Lasota 2001). Persistent systems may be accreting at close to the mass transfer rate, thus preventing both the build-up and depletion of mass in the disk. It may also be that a high mass transfer rate keeps the outer disk ionized, hence driving the observed persistent accretion rate over long periods of time (Lasota 2001; in't Zand et al. 2007). This accretion rate would be lower than in most transient systems during outburst but also higher than typical quiescent ones. This is especially relevant for UCXBs where the mass transfer rate is driven by gravitational wave radiation (van Haaften et al. 2012), resulting in high mass transfer rates for a low-mass donor star overflowing its Roche lobe.

Following van Haaften et al. (2012) for ultracompact systems, and assuming that the 2−10 keV X-ray luminosity is half of the bolometric luminosity of 4U 1556–60 (Anastasopoulou et al. 2022), we estimate that the mass transfer rate from the donor to the disk is 2×10^{-11} $M_\odot$/year (10^{15} g/s) for a neutron star accretor. This mass transfer rate for a white dwarf donor driven by gravitational wave radiation corresponds to an orbital period of 20−30 minutes (Fig. 2 in van Haaften et al. 2012), and again points toward an ultracompact nature for 4U 1556–60.

4U 1556–60's X-ray luminosity is indeed similar to a 28 minute ultracompact candidate BHXB that appears to be in an unusually bright quiescence of $L_X \gtrsim 10^{33}$ erg s^{-1}, 47 Tuc X9 (Bahramian et al. 2017). This persistent luminosity is believed to be driven by an elevated mass transfer rate from the degenerate donor in quiescence. A similar scenario is theorized for the persistent NSXB RX J1718.4–4029 (in't Zand et al. 2009), which has an X-ray luminosity of ~8×10^{34} erg s^{-1}, though an orbital period has not been confirmed in this system. The confirmed NS UCXB IGR J17062–6143 (Strohmayer et al. 2018) was discovered during an outburst in 2006 (Churazov et al. 2007), and has since resided at a persistent luminosity of ~10^{35} erg s^{-1}, a particularly high non-outburst value for a transient system.

Systems such as these with L_X of 10^{34-35} erg s^{-1} are known as very faint X-ray binaries (VFXBs) (e.g., Pavlinsky et al. 1994; Heinke et al. 2015). Many VFXBs are also UCXBs, though giant donor stars have also been identified in two NS VFXBs (Shaw et al. 2020, 2024). However, the faintness of the OIR counterpart effectively rules out a giant donor scenario for 4U 1556–60 at any Galactic distance.

4.2.4. Presence of hydrogen

The presence of hydrogen in one optical spectrum is notable given that 4U 1556–60 is estimated above to be ultracompact, limiting the potential orbital period and evolution history. The apparently variable strength of hydrogen lines (very weak but present in Motch et al. 1989, and strongly found later in Nelemans et al. 2006) could indicate that there is a small amount of hydrogen in the accretion disk, such that small fluctuations in ionization lead to large changes in the strength of the Balmer lines. Thus, an ultracompact system with trace amounts of hydrogen in the donor star is a possibility for 4U 1556–60.

Hydrogen is very problematic for UCXBs that have very short orbital periods of ≲20 minutes (e.g., Podsiadlowski et al. 2003; Belloni & Schreiber 2023), but is possible for slightly longer ones. Based on simulations of white dwarf accretors, it is indeed possible for a small fraction of hydrogen to remain in the donor envelope at short orbital periods if the donor is an evolved star rather than a white dwarf (Nelemans et al. 2010; Goliasch & Nelson 2015; Kalomeni et al. 2016). This scenario is similar to the 51 minute accreting white dwarf system ZTF J1813+4251 (Burdge et al. 2022), which has observed hydrogen lines and is expected to reach a minimum orbital period of ~20 minutes. Thus, it is perhaps more likely that 4U 1556–60 has an orbital period that is greater than 20 minutes, such that the donor is an evolved star that has not yet been fully stripped of hydrogen, and the binary is currently evolving toward a period minimum. In this case, 4U 1556–60 would likely be the product of two common envelope phases. A UCXB with an evolved donor should be a rare occurrence; if this scenario is indeed true, 4U 1556–60 being the only known member of this

class is unsurprising given that there are only about 50 known or candidate UCXBs to date.

4.2.5. Inclination angle

No eclipsing or dipping features in the X-ray light curve have been observed, indicating that 4U 1556–60 is not highly inclined. A further estimation of its inclination angle can be performed by utilizing its optical spectrum. We take the full width at half maximum (FWHM) of the strong hydrogen line in Nelemans et al. (2006) of 540 km s^{-1} and use the relation of Casares (2015) between the FWHM of Hα and K2 (the orbital velocity of the donor star) to estimate the required inclination angle given a constraint on the orbital period. For an orbital period of 30 minutes, i is 8°, for 1 hour it is 11°, and for a much longer period of 6 hours it is still only 20° (nominal errors of ±3°). Thus, 4U 1556–60 is likely a low inclination system for any reasonable orbital period based on its observed narrow Hα line.

4.2.6. A mHz gravitational wave source

Lastly, we briefly consider that a UCXB at a distance of 700 pc is a very appealing prospect for mHz gravitational wave (GW) detection in the future, such as with the Laser Interferometer Space Antenna (LISA; Amaro-Seoane et al. 2017). UCXBs are one of the anticipated sources of mHz GWs (Nelemans 2009; Chen et al. 2020), where mHz GW detectors may detect many systems that are currently not known from electromagnetic observations. Simulations indicate that $O(5)$ UCXBs that evolved from the main sequence channel should be detectable as mHz GW sources (Chen & Liu 2025), as we suggest is the evolution scenario for 4U 1556–60. Using `LEGWORK` (Wagg et al. 2022), 4U 1556–60 will be detectable at 5σ with LISA in 4 years if the orbital period and donor star mass are, for example: 20 min and $\gtrsim$0.013 M$_\odot$; 30 min and $\gtrsim$0.05 M$_\odot$; or 60 min and $\gtrsim$0.3 M$_\odot$, respectively. Thus, it is possible that 4U 1556–60 will be a detectable mHz GW source if its orbital period is sufficiently short; the donor mass requirements for the shorter orbital periods in particular are indeed reasonable and similar to estimates for known UCXBs (e.g., Heinke et al. 2013). A stricter estimate of its strain will be possible when an orbital period is confirmed or better constrained for 4U 1556–60, at which time it may become a candidate verification binary for LISA and other mHz GW detectors.

4.3. X-ray spectral and timing features

4.3.1. X-ray spectrum

The blackbody spectral component corresponds to a small emitting area of a 0.21 ± 0.02 km radius from the normalization of `bbodyrad`. This is much smaller than the size of a neutron star, and is also inconsistent with a black hole accretor. This suggests either a hotspot most likely located on the magnetic pole, or a thin boundary or spreading layer belt. The former scenario may indicate a somewhat strong magnetic field that channels the accreting matter onto the magnetic pole. Combining this with the lack of a spin period found in the timing analysis then suggests a scenario where the obliquity angle between the spin and magnetic axes is small such that the hotspot flux remains largely unmodulated by the spin of the NS. The latter scenario is a small boundary or spreading layer that produces the thermal emission. The lack of a hotspot spectral component then may indicate that the magnetic field is weak as in most LMXBs, and thus that the neutron star likely has a ∼milliseconds spin period.

The X-ray spectrum overall is very consistent with typical hard state LMXBs. NSXBs with very strong magnetic fields show flatter power laws than we find here in 4U 1556–60 (White et al. 1983), thus spectrally it is unlikely that there is a very strong magnetic field of $\gtrsim 10^{12}$ G, independent of the lack of detected pulsations.

The weak iron line detected in the NICER spectrum with an equivalent with of 8 eV is a notable feature. There are a few reasons why there may be a weak iron line in an XRB: (1) a highly ionized disk; (2) a disk that is truncated far from the accretor; and (3) high abundances of carbon or oxygen that screen the iron fluorescence (Koliopanos et al. 2013). We can safely rule out a highly ionized disk given the low X-ray luminosity of 4U 1556–60. A truncated accretion disk is possible and rather expected given the low accretion rate, and that we do not find a reasonable accretion disk component to be present in the X-ray spectrum. High carbon or oxygen abundances are also possible if the system is a UCXB with a carbon- or oxygen-rich donor. Given that the X-ray spectrum is not reasonably fit with a `diskbb`, we can attribute the weak iron line feature to a truncated accretion disk, which has been observed in other NSXBs at low luminosities (e.g., Degenaar et al. 2017; van den Eijnden et al. 2020). This reinforces that 4U 1556–60 is accreting at a very low rate which is only possible at a very close distance given its X-ray flux. A carbon- or oxygen-rich donor may also be feasible in addition to a truncated accretion disk.

Spectral investigations of UCXBs have found both strong (e.g., Degenaar et al. 2017, notably at a low L_X of ∼10^{35} erg s^{-1}) and undetected (e.g., Campana et al. 2003; Miller et al. 2003; Sanna et al. 2018) iron lines, as well as long-term variable iron line strengths (Koliopanos et al. 2021), uncorrelated with luminosity or spectral state. Therefore, the weak iron line here in 4U 1556–60 is inconclusive for the UCXB population especially given the inferred truncated disk above.

4.3.2. X-ray timing properties

First, we further discuss the nondetection of a pulse period of <1%, which has some relevance to the NS magnetic field. Many NS LMXBs do not have known spin periods, so this is not unusual. Pulsations are likely due to moderately strong magnetic fields ($B \gtrsim 10^9$ G) that are able to channel accreting material and create hotspots on the NS surface (Bildsten et al. 1997; Patruno & Watts 2021). Furthermore, of the systems that do show pulsations, some have only sporadically detected epochs of pulsations (e.g., Altamirano et al. 2008; Casella et al. 2008). The reasons governing why pulsations appear in some systems during certain times is not clear. Thus, we cannot rule out a moderately strong magnetic field similar to accreting millisecond X-ray pulsars (Wijnands & van der Klis 1998), though a very strong field ($B \geq 10^{12}$ G) is highly unlikely.

Other X-ray timing features of 4U 1556–60 point toward a very low accretion rate. The fractional RMS of the NICER data is 25%, which is comparable to observations of hard states and is much higher than the low RMS of a few percent during soft states (Muñoz-Darias et al. 2011). The turnover frequency of the power spectrum of the very low frequency noise (VLFN) component is observationally positively correlated to the X-ray luminosity, and thus accretion rate (e.g., Reig et al. 2004; Armas Padilla et al. 2014). We find that there is no turnover observed in 4U 1556–60 down to ∼10^{-3} Hz (Fig. 7, left). The NSXB Aql X–1 had an observed turnover at a frequency of

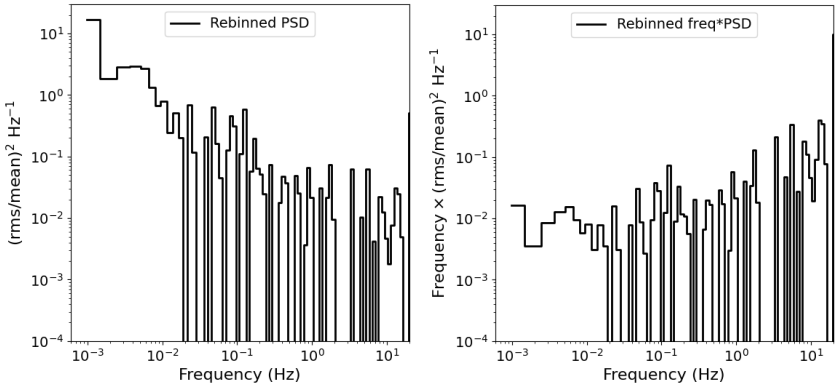

Fig. 7. Averaged power spectrum of 4U 1556–60 of NICER data from `stingray`. On the left, the PSD shows a very low frequency noise component that remains unbroken to at least near 10^{-3} Hz. This is a very low frequency constraint on the break frequency value compared to other XRBs, an indication of a low intrinsic X-ray luminosity. On the right, the fractional power of 10^{-2} is also consistent with low accretion rate hard states in other XRBs, and is much higher than during soft states.

0.1 Hz at an X-ray luminosity of $\sim 7 \times 10^{35}$ erg s^{-1} (Reig et al. 2004), and the very faint BHXB transient Swift J1357.2−0933 had an observed turnover at 0.01 Hz at an X-ray luminosity of $\sim 10^{35}$ erg s^{-1} (Armas Padilla et al. 2014). The fractional power of both systems was about 10^{-2}, consistent with the fractional power observed in 4U 1556–60 (Fig. 7, right). The lack of an observed turnover in the PSD suggests that 4U 1556–60's X-ray luminosity is likely similar to or lower than the observations of the systems above.

4.4. Radio jet

A correlation between the X-ray and radio luminosities of XRBs is observed, particularly well in BHXBs (Fender et al. 2004; Gallo et al. 2018) (Fig. 5), indicative of disk-jet coupling behavior and generally fit with a power law slope parameter β. BHXBs follow a close correlation across a wide range of X-ray luminosities, with $\beta \simeq 0.7$ (Gallo et al. 2006, 2018). However, it is less clear to date how NSXBs are correlated as there is a much wider range of radio luminosities for these systems. There have indeed been different β values estimated for different classes of NSXBs, as well as among different NSXBs in the same class, ranging from $\simeq$0.4 to $\simeq$1.5 (Qiao & Liu 2019), suggesting additional disk-jet complexity compared to BHXBs. The radio luminosity normalization of NSXBs is certainly lower on average than BHXBs (by a factor of $\sim$22; Gallo et al. 2018) and spans at least two orders of magnitude across observed NSXBs to date (van den Eijnden et al. 2021), and may depend on factors such as the NS's intrinsic magnetic field strength and its spin (e.g., van den Eijnden et al. 2018).

As discussed before, the upper limit on 4U 1556–60's radio luminosity of $\sim 3 \times 10^{25}$ erg s^{-1} strongly indicates that the accretor is a NS rather than a BH, as this value is about 3 orders of magnitude fainter than the BHXB correlation at a similar X-ray luminosity of 10^{34} erg s^{-1}. There are also numerous radio jet detections of BHXBs at similar and lower X-ray luminosities as seen in Fig. 5. Thus, a jet is expected to be present in 4U 1556–60 due to its hard spectral state, and be easily detectable by our high-sensitivity radio observation if this system contained a BH accretor.

Our radio nondetection leaves two general possibilities for the jet of 4U 1556–60 with the assumption that it is a NSXB. One is that there is indeed a jet being produced that is very weak and thus undetected, through a steep β slope, a low radio normalization factor (see Fig. 5), or a combination of both. The other is that there is no jet being produced in this low accretion rate NSXB. Some BHXBs have confirmed radio emission during quiescence, attributed to a radio jet (Gallo et al. 2014); however, no quiescent ($L_X \simeq 10^{32}$ erg s^{-1}) NSXB has been detected in radio, thus the existence of radio jets in any class of NSXBs down to very low accretion rates remains unclear. It may be possible that at low accretion rates, the NS magnetosphere is able to quench the jet production in some way; that is, that there is a β correlation above some L_X and a steep drop below it, but to date this is unknown.

It is also notable that there are indeed NSXB radio detections at higher radio luminosities for similar X-ray luminosities as 4U 1556–60. These are either accreting millisecond X-ray pulsars (AMXPs; Wijnands & van der Klis 1998), or transitional millisecond pulsars (tMSPs; Archibald et al. 2009). AMXPs have higher magnetic field strengths than the general NS LMXB population as evidenced by their X-ray pulsations, and tMSPs are a rare and less understood type of NSXB where the radio emission during their XRB phase does not behave as expected of a canonical compact jet (Bogdanov et al. 2018) (perhaps due to a propeller regime; Illarionov & Sunyaev 1975). There is no evidence that 4U 1556–60 is a tMSP (Papitto & de Martino 2022), as it is a persistent XRB without the characteristic step-function-shaped X-ray light curve of tMSPs, and is neither a radio nor gamma-ray source. The radio jets of AMXPs are puzzling, as they host some of the brightest and faintest NSXB radio jets relative to their X-ray luminosities (Tetarenko et al. 2016; Tudor et al. 2017), thus a comparison of 4U 1556–60's radio jet luminosity limit to AMXP observations at similar X-ray luminosities is also not revealing.

A compilation of radio emission from a number of UCXBs by Tetarenko et al. (2018) and recently expanded with new observations by Dage et al. (2025) do not find a correlation between orbital period and radio luminosity within the UCXB population. The radio luminosities of UCXBs are consistent with the longer period population of LMXBs as well. Thus, to date there is no correlation between radio luminosity and orbital period of XRBs. This may indeed be expected as the jets are theoretically launched by magnetic fields in the vicinity of the accretor (Blandford & Znajek 1977; Blandford & Payne 1982), which are not correlated with the size of the accretion disk, though there may also be some effect on jet production due to the altered mass:charge ratio of hydrogen-poor accretion disk material feeding the jet. Therefore, we are unable to draw a conclusion about 4U 1556–60's orbital period based on its radio nondetection.

Interestingly, there has been a NS UCXB observed to display drastic radio luminosity fluctuations, X1850–087 (Panurach et al. 2023). This is a persistent system with $L_X \simeq 10^{36}$ erg s^{-1}, and its radio jet was observed to vary significantly by a factor of >10 despite only small changes in the X-ray lumi-

nosity over several days. The cause of this radio variability is not known definitively, but it was suggested that there may be strong jet quenching below some L_X value. This is similar to one of the scenarios we have considered for the very low L_R upper limit of 4U 1556–60. Though, there is no indication that this jet variability is related to a UCXB nature, as there may also be some similarities with longer period AMXPs discussed above.

The very low radio luminosity limit of 4U 1556–60 due to its close distance has provided a strong constraint in new $L_R - L_X$ parameter space on the behavior of some NSXB jets at low X-ray luminosities, and motivates further deep radio monitoring of similar systems to better fill in the luminosity gap between 4U 1556–60 and the majority of the radio-detected NSXB population at higher X-ray luminosities.

4.5. Considering a longer orbital period or larger distance

Here we consider whether the orbital period of 4U 1556–60 might not be ultracompact and instead may be a more common LMXB value of a few hours, and whether it may be located at a distance much greater than 700 pc.

4.5.1. A longer orbital period at 700 pc

The immediate difficulty with an orbital period longer than ∼2 hours is the faintness of the OIR counterpart, and the infrared one in particular as discussed in Section 4.2.1. A longer orbital period would necessitate that the donor star be significantly underluminous while filling its Roche lobe, which is unreasonable. Therefore, if 4U 1556–60 is indeed located at its *Gaia* parallax distance, its orbital period cannot be longer than about 2 hours, and it should indeed be shorter than this when considering that the disk contributes significantly to the OIR emission.

4.5.2. At a Galactic Center distance

Another possibility is that the *Gaia* parallax is either not accurate, or is affected by an interloper star such that the distance to 4U 1556–60 is significantly larger than 700 pc. These are unlikely given the $>5\sigma$ parallax, the consistency of the proper motion, and the extremely low probability of either dwarf stars or white dwarfs superimposed on the *Gaia* counterpart. However, if 4U 1556–60 is indeed located at a larger distance, the optical luminosity will increase, which allows for a nominally brighter and larger companion star and thus longer orbital period based on the OIR luminosity alone.

At a larger distance of, for example, 7 kpc, the radio nondetection is notable again. 4U 1556–60 would be one of the lowest radio upper limits for an XRB with $L_R \lesssim 3 \times 10^{27}$ erg s^{-1} at similar X-ray luminosities of $L_X \simeq 10^{36}$ erg s^{-1} (Fig. 5). It would again lie in a parameter space that is outside of the observed range of $L_R - L_X$ for BHXBs (this includes the radio-faint BHXB track at similar X-ray luminosities; Coriat et al. 2011), indicating a NS accretor regardless of its distance.

The X-ray luminosity at 7 kpc becomes a more commonly observed persistent XRB value of $\sim 10^{36}$ erg s^{-1}. The X-ray spectral and timing features remain the same; that is, the accretion rate must be consistent with a hard spectral state, which is reasonable if $L_X \simeq 10^{36}$ erg s^{-1} or 1% L_{Edd}. The thermal X-ray spectral component is still not compatible with a disk due to the inner radius remaining much smaller than the size of a neutron star (disk inner radius from the normalization parameter of up to 2 km at 7 kpc). The vPM94 orbital period estimation is also affected, where the orbital period increases with distance, for example, to a nominal value of 1.1±0.9 hours at 7 kpc (6±5 hours at +0.5 log Σ). At an orbital period of a few hours, hydrogen is indeed expected in the spectrum, and the inclination angle estimations are the same.

There is indeed a concern though, as an increased distance and thus X-ray luminosity also raises the issue of the burst rate again. During hard states at 10^{36} erg s^{-1}, NS LMXBs routinely burst every few hours or so (e.g., Cornelisse et al. 2003; Galloway et al. 2020) as the elevated mass accretion rate onto the NS quickly builds up a layer of hydrogen or helium to critical mass and temperature for ignition. As discussed above, there are no indications that 4U 1556–60 has a very strong magnetic field that would inhibit bursting behavior, and it being an LMXB generally disfavors a highly magnetized scenario as well due to the presumed recycling of the NS accretor (Bhattacharya & van den Heuvel 1991; Wijnands & van der Klis 1998) (though there is also a known highly magnetized NS UCXB, the 7.7 s pulsar 4U 1626–67; Middleditch et al. 1981; Orlandini et al. 1998). However, due to the lack of evidence that 4U 1556–60 hosts a strong magnetic field, we assume that it does not and thus there is no reason that it would not be frequently bursting at a luminosity of 10^{36} erg s^{-1} at a distance of several kpc with a helium- and possibly hydrogen-rich donor. This is a serious issue which strongly indicates that 4U 1556–60 cannot be at a larger distance of several kpc, regardless of its orbital period at that distance.

4.5.3. On the far side of the Galaxy

A final consideration is if 4U 1556–60 might be much further away than the Galactic Center, and may possibly be a halo object. There are indeed a couple of LMXBs with distances estimated to be >20 kpc (Casares et al. 2004; Homan et al. 2011). At a distance of 20 kpc, $L_X \simeq 10^{37}$ erg s^{-1} or 10% L_{Edd}, which is on the border between hard and soft states in XRBs (e.g., Barret et al. 1996). A soft accretion state would significantly ease the tension with the burst rate or the radio nondetection; however, as discussed above, the timing (strong variability) and spectral (nonthermal-dominated) properties of the X-ray data clearly indicate a hard state. Thus, requiring that 4U 1556–60 be in a hard state effectively limits its distance to $\lesssim$20 kpc. Then again, in a hard state similar to the 7 kpc case above, there is a severe issue with the lack of thermonuclear bursts for a NSXB actively accreting at a relatively high rate with a presumed hydrogen- and helium-rich donor star.

5. Summary

The *Gaia* parallax distance in combination with old and new data have enabled a fresh look at the parameters of 4U 1556–60, and a very faint ultracompact NSXB at ∼700 pc interpretation is able to explain many of its observed characteristics. We summarize our various findings below.

5.1. Basic properties

- *Gaia* has determined the distance of the optical counterpart of 4U 1556–60 to be ∼700 pc with no evidence of, and a very low probability for, an interloper star. This is one of the closest X-ray binaries known to date, and is the closest known Roche lobe overflowing LMXB.
- The X-ray luminosity is stably around 2×10^{34} erg s^{-1}, an unusually low luminosity for a persistent system, or alterna-

tively an unusually bright quiescence. MAXI and targeted X-ray data indicate that there has been no significant long-term X-ray variability of 4U 1556–60 since its discovery more than 50 years ago, including no outbursts.
– New radio data have provided a deep upper limit for 4U 1556–60's radio jet, and it is about 3 orders of magnitude fainter than the BHXB correlation in $L_R - L_X$ and well below the scatter of the BHXBs. This almost certainly determines that 4U 1556–60 hosts a neutron star accretor.

5.2. Binary orbit and companion or composition

– The optical and infrared luminosities are extremely low, thus the orbital period must be very short, and is likely to be ultracompact. The X-ray and optical luminosities following van Paradijs & McClintock (1994), as well as with the infrared counterpart following Russell et al. (2006), broadly indicate a very short orbital period of a few to tens of minutes. The infrared counterpart alone also conservatively restricts the orbital period to a maximum of ∼2 hours.
– There have been hydrogen emission disk lines observed in the optical spectrum, though the strength varied significantly in two separate observations. A UCXB may have residual hydrogen if the donor is an evolved star, which is a rare evolutionary channel for UCXBs.
– Using the Hα FWHM-K2 relation of Casares (2015), we determine that 4U 1556–60 must be oriented at a very low inclination angle for any reasonable orbital period. This would also explain the lack of an observed orbital periodicity in the NICER data.

5.3. X-ray results

– The X-ray spectrum is fit with a power law and blackbody component. A disk blackbody results in an unphysical inner disk radius, thus the spectrum is consistent with a truncated accretion disk, also aligning with the low accretion rate and potentially the effect of a NS magnetosphere. The small blackbody component is also inconsistent with a black hole accretor.
– There is a weak iron line with an equivalent width of ∼8 eV. This can be explained by a truncated accretion disk, in line with the spectroscopic results.
– An additional explanation for both the weak iron line and lack of bursts is that the accretion disk may have significant abundances of carbon or oxygen. This would be expected if 4U 1556–60 has a very short orbital period and thus a carbon- or oxygen-rich donor star, as suggested above, though the low X-ray luminosity is sufficient to explain both of these findings regardless of the composition of the disk.
– There is no indication of an orbital ($5\sigma < 2$–5%) or spin period ($5\sigma < 1\%$) in recent X-ray data. The lack of an orbital period can be explained by a low inclination angle, and the lack of a spin period suggests either that the NS accretor has a weak magnetic field as is common in NS LMXBs, or that the spin and magnetic axes are closely aligned.
– The X-ray power spectrum is dominated by a very low frequency noise component commonly observed in hard state XRBs, and the break frequency is constrained to be $\lesssim 10^{-3}$ Hz. This is a very low value, which suggests that the X-ray luminosity is intrinsically very low, and is lower than typical hard state NSXB observations at $\sim 10^{36}$ erg s^{-1}.
– No Type I bursts have been observed from 4U 1556–60 despite its NS nature, which can also now be explained by its very low accretion rate with predicted recurrence times on the order of months to years. If it does burst, it may be a rare and bright intermediate duration burst.

5.4. Radio and other results

– The radio jet is undetected with an upper limit of 5×10^{25} erg s^{-1}, one of the lowest radio upper limits obtained for an XRB, with two general possibilities. One is that a jet is present but much weaker than some AMXPs and tMSPs at similar X-ray luminosities. We rule out 4U 1556–60 being a tMSP, but are unable to draw a conclusion about similarities with AMXPs. The other is that at this low accretion rate, there is NS magnetospheric jet quenching regardless of the β slope or normalization parameter in $L_R - L_X$, which is not observed in BHXBs. This may be a vital clue as to the ability of NSXBs to launch jets at very low accretion rates.
– A persistently active XRB at a low X-ray luminosity is more easily sustained in a shorter orbital period system than a longer one, as it is easier to keep a physically small accretion disk ionized, thus also mildly supporting an ultracompact nature. Alternatively, a persistent low, but higher than quiescent, X-ray luminosity has been observed in other UCXBs, possibly due to an elevated mass transfer rate from a degenerate donor due to gravitational wave radiation.
– It may be possible that 4U 1556–60 is at a much larger distance if the *Gaia* parallax is incorrect. In this case the radio nondetection still indicates a NS accretor, with an upper limit of ∼20 kpc for it to remain spectrally in a hard state. However, the lack of bursting at a higher X-ray luminosity with a helium-rich and presumed hydrogen-rich donor is not able to be explained, and a black hole accretor is still unreasonable. Placing 4U 1556–60 at a larger distance seems more problematic than at 700 pc.
– A UCXB at 700 pc is a promising future mHz gravitational wave source if its orbital period is sufficiently short. A future detection of 4U 1556–60's orbital period will allow for a more accurate estimate of its strain.

4U 1556–60 has become an intriguing XRB in light of recent data, and we have formed a novel interpretation that explains many previous uncertainties regarding this system and its properties. We have determined that 4U 1556–60 is located at a distance of only ∼700 pc from its *Gaia* parallax, the closest low-mass Roche lobe overflowing XRB known to date. It is a NSXB existing at an unusual persistent X-ray luminosity of 2×10^{34} erg s^{-1}, though it has never been observed to burst which is now explainable by its very low accretion rate. It is very likely to be an ultracompact system due to its high X-ray:optical flux ratio and overall faint OIR counterpart, though still with residual hydrogen in its disk. It hosts a very weak or absent radio jet, for which we have obtained an upper limit at one of the lowest radio luminosities ever observed in an XRB, and in an unprecedented parameter space on $L_R - L_X$. Its close proximity will be beneficial to multiwavelength follow-up in the near future to better refine various parameters, and particularly to identify its orbital period to confirm the theory of 4U 1556–60 presented here.

Acknowledgements. We thank the anonymous referee for providing useful suggestions which improved the manuscript. This research has made use of data and/or software provided by the High Energy Astrophysics Science Archive Research Center (HEASARC), which is a service of the Astrophysics Science Division at NASA/GSFC. The Australia Telescope Compact Array is part of

the Australia Telescope National Facility (grid.421683.a) which is funded by the Australian Government for operation as a National Facility managed by CSIRO. ECP and TJM acknowledge funding via the NICER Guest Observer program, through grant 80NSSC23K1119. This research was supported by Deutsche Forschungsgemeinschaft (DFG, German Research Foundation) under Germany's Excellence Strategy – EXC 2121 "Quantum Universe" – 390833306. Co-funded by the European Union (ERC, CompactBINARIES, 101078773). Views and opinions expressed are however those of the author(s) only and do not necessarily reflect those of the European Union or the European Research Council. Neither the European Union nor the granting authority can be held responsible for them. We acknowledge the Gomeroi people as the traditional owners of the ATCA observatory site. We thank Jakob van den Eijnden, Duncan K. Galloway, James C. A. Miller-Jones, and Anna L. Watts for useful discussions.

References

Alizai, K., Chenevez, J., Cumming, A., et al. 2023, MNRAS, 521, 3608
Altamirano, D., Casella, P., Patruno, A., Wijnands, R., & van der Klis, M. 2008, ApJ, 674, L45
Amaro-Seoane, P., Audley, H., Babak, S., et al. 2017, ArXiv e-prints [arXiv:1702.00786]
Anastasopoulou, K., Zezas, A., Steiner, J. F., & Reig, P. 2022, MNRAS, 513, 1400
Anders, E., & Grevesse, N. 1989, Geochim. Cosmochim. Acta, 53, 197
Archibald, A. M., Stairs, I. H., Ransom, S. M., et al. 2009, Science, 324, 1411
Armas Padilla, M., Wijnands, R., Altamirano, D., et al. 2014, MNRAS, 439, 3908
Armas Padilla, M., Corral-Santana, J. M., Borghese, A., et al. 2023, A&A, 677, A186
Arnason, R. M., Papei, H., Barmby, P., Bahramian, A., & Gorski, M. D. 2021, MNRAS, 502, 5455
Arnaud, K. A. 1996, ASP Conf. Ser., 101, 17
Astropy Collaboration (Robitaille, T. P., et al.) 2013, A&A, 558, A33
Avakyan, A., Neumann, M., Zainab, A., et al. 2023, A&A, 675, A199
Bahramian, A., & Rushton, A. 2022, https://doi.org/10.5281/zenodo.7059313
Bahramian, A., Heinke, C. O., Tudor, V., et al. 2017, MNRAS, 467, 2199
Bailer-Jones, C. A. L., Rybizki, J., Fouesneau, M., Demleitner, M., & Andrae, R. 2021, AJ, 161, 147
Barret, D., McClintock, J. E., & Grindlay, J. E. 1996, ApJ, 473, 963
Barthelmy, S. D., Barbier, L. M., Cummings, J. R., et al. 2005, Space Sci. Rev., 120, 143
Belloni, D., & Schreiber, M. R. 2023, A&A, 678, A34
Bhattacharya, D., & van den Heuvel, E. P. J. 1991, Phys. Rep., 203, 1
Bildsten, L., Chakrabarty, D., Chiu, J., et al. 1997, ApJS, 113, 367
Blandford, R. D., & Payne, D. G. 1982, MNRAS, 199, 883
Blandford, R. D., & Znajek, R. L. 1977, MNRAS, 179, 433
Bogdanov, S., Deller, A. T., Miller-Jones, J. C. A., et al. 2018, ApJ, 856, 54
Burdge, K. B., El-Badry, K., Marsh, T. R., et al. 2022, Nature, 610, 467
Campana, S., Ravasio, M., Israel, G. L., Mangano, V., & Belloni, T. 2003, ApJ, 594, L39
CASA Team (Bean, B., et al.) 2022, PASP, 134, 114501
Casares, J. 2015, ApJ, 808, 80
Casares, J., Zurita, C., Shahbaz, T., Charles, P. A., & Fender, R. P. 2004, ApJ, 613, L133
Casella, P., Altamirano, D., Patruno, A., Wijnands, R., & van der Klis, M. 2008, ApJ, 674, L41
Charles, P. A., Thorstensen, J. R., Bowyer, S., et al. 1979, BAAS, 11, 720
Chen, M., & Liu, J. 2025, ApJ, 981, 175
Chen, W.-C., Liu, D.-D., & Wang, B. 2020, ApJ, 900, L8
Churazov, E., Sunyaev, R., Revnivtsev, M., et al. 2007, A&A, 467, 529
Cocchi, M., Bazzano, A., Natalucci, L., et al. 2001, A&A, 378, L37
Corbel, S., Koerding, E., & Kaaret, P. 2008, MNRAS, 389, 1697
Coriat, M., Corbel, S., Prat, L., et al. 2011, MNRAS, 414, 677
Cornelisse, R., Verbunt, F., in't Zand, J. J. M., Kuulkers, E., & Heise, J. 2002, A&A, 392, 931
Cornelisse, R., in't Zand, J. J. M., Verbunt, F., et al. 2003, A&A, 405, 1033
Cruz, K. L., Reid, I. N., Kirkpatrick, J. D., et al. 2007, AJ, 133, 439
Dage, K. C., Panurach, T., Oh, K., et al. 2025, ApJ, 988, 131
Degenaar, N., Jonker, P. G., Torres, M. A. P., et al. 2010, MNRAS, 404, 1591
Degenaar, N., Pinto, C., Miller, J. M., et al. 2017, MNRAS, 464, 398
Degenaar, N., Ballantyne, D. R., Belloni, T., et al. 2018, Space Sci. Rev., 214, 15
Done, C., Gierliński, M., & Kubota, A. 2007, A&ARv, 15, 1
Dubus, G., Lasota, J.-P., Hameury, J.-M., & Charles, P. 1999, MNRAS, 303, 139
Duldig, M. L., Greenhill, J. G., Thomas, R. M., et al. 1979, MNRAS, 187, 567
Farinelli, R., Masetti, N., Frontera, F., et al. 2003a, ASP Conf. Ser., 308, 283
Farinelli, R., Frontera, F., Masetti, N., et al. 2003b, A&A, 402, 1021
Fender, R. P. 2001, MNRAS, 322, 31
Fender, R. P., Belloni, T. M., & Gallo, E. 2004, MNRAS, 355, 1105
Gaia Collaboration (Vallenari, A., et al.) 2023, A&A, 674, A1
Gallo, E., Fender, R. P., Miller-Jones, J. C. A., et al. 2006, MNRAS, 370, 1351
Gallo, E., Miller-Jones, J. C. A., Russell, D. M., et al. 2014, MNRAS, 445, 290
Gallo, E., Degenaar, N., & van den Eijnden, J. 2018, MNRAS, 478, L132
Galloway, D. K., Zand, J., Chenevez, J., et al. 2020, ApJS, 249, 32
Gandhi, P., Rao, A., Johnson, M. A. C., Paice, J. A., & Maccarone, T. J. 2019, MNRAS, 485, 2642
Gendreau, K. C., Arzoumanian, Z., Adkins, P. W., et al. 2016, SPIE Conf. Ser., 9905, 99051H
Gentile Fusillo, N. P., Tremblay, P. E., Cukanovaite, E., et al. 2021, MNRAS, 508, 3877
Giacconi, R., Murray, S., Gursky, H., et al. 1972, ApJ, 178, 281
Goliasch, J., & Nelson, L. 2015, ApJ, 809, 80
Hawley, S. L., Covey, K. R., Knapp, G. R., et al. 2002, AJ, 123, 3409
Heinke, C. O., Grindlay, J. E., Lugger, P. M., et al. 2003, ApJ, 598, 501
Heinke, C. O., Rybicki, G. B., Narayan, R., & Grindlay, J. E. 2006, ApJ, 644, 1090
Heinke, C. O., Ivanova, N., Engel, M. C., et al. 2013, ApJ, 768, 184
Heinke, C. O., Bahramian, A., Degenaar, N., & Wijnands, R. 2015, MNRAS, 447, 3034
Homan, J., Linares, M., van den Berg, M., & Fridriksson, J. 2011, ATel, 3650, 1
Huppenkothen, D., Bachetti, M., Stevens, A. L., et al. 2019, ApJ, 881, 39
Illarionov, A. F., & Sunyaev, R. A. 1975, A&A, 39, 185
in't Zand, J. J. M., Jonker, P. G., & Markwardt, C. B. 2007, A&A, 465, 953
in't Zand, J. J. M., Jonker, P. G., Bassa, C. G., Markwardt, C. B., & Levine, A. M. 2009, A&A, 506, 857
in't Zand, J. J. M., Kries, M. J. W., Palmer, D. M., & Degenaar, N. 2019, A&A, 621, A53
Ivanova, N., Heinke, C. O., Rasio, F. A., Belczynski, K., & Fregeau, J. M. 2008, MNRAS, 386, 553
Jenke, P. A., Linares, M., Connaughton, V., et al. 2018, VizieR Online Data Catalog: J/ApJ/826/228
Joss, P. C., & Li, F. K. 1980, ApJ, 238, 287
Kalomeni, B., Nelson, L., Rappaport, S., et al. 2016, ApJ, 833, 83
Koliopanos, F., Gilfanov, M., & Bildsten, L. 2013, MNRAS, 432, 1264
Koliopanos, F., Vasilopoulos, G., Guillot, S., & Webb, N. 2021, MNRAS, 500, 5603
Kuulkers, E., in't Zand, J. J. M., & Lasota, J.-P. 2009, A&A, 503, 889
Lasota, J.-P. 2001, New Astron. Rev., 45, 449
Lewin, W. H. G., van Paradijs, J., & Taam, R. E. 1993, Space Sci. Rev., 62, 223
Lin, J., & Yu, W. 2020, ApJ, 903, 37
Linares, M., Connaughton, V., Jenke, P., et al. 2012, ApJ, 760, 133
Matsuoka, M., Kawasaki, K., Ueno, S., et al. 2009, PASJ, 61, 999
McMahon, R. G., Banerji, M., Gonzalez, E., et al. 2013, The Messenger, 154, 35
Meegan, C., Lichti, G., Bhat, P. N., et al. 2009, ApJ, 702, 791
Middleditch, J., Mason, K. O., Nelson, J. E., & White, N. E. 1981, ApJ, 244, 1001
Miller, J. M., Wijnands, R., Méndez, M., et al. 2003, ApJ, 583, L99
Motch, C., Chevalier, C., Ilovaisky, S. A., & Pakull, M. W. 1985, Space Sci. Rev., 40, 239
Motch, C., Pakull, M. W., Mouchet, M., & Beuermann, K. 1989, A&A, 219, 158
Muñoz-Darias, T., Motta, S., & Belloni, T. M. 2011, MNRAS, 410, 679
Nasa High Energy Astrophysics Science Archive Research Center (Heasarc) 2014, Astrophysics Source Code Library [record ascl:1408.004]
Nelemans, G. 2009, Class. Quant. Grav., 26, 094030
Nelemans, G., Yungelson, L. R., & Portegies Zwart, S. F. 2001, A&A, 375, 890
Nelemans, G., Jonker, P. G., & Steeghs, D. 2006, MNRAS, 370, 255
Nelemans, G., Yungelson, L. R., van der Sluys, M. V., & Tout, C. A. 2010, MNRAS, 401, 1347
Orlandini, M., Dal Fiume, D., Frontera, F., et al. 1998, ApJ, 500, L163
Paczynski, B. 1976, IAU Symp., 73, 75
Panurach, T., Urquhart, R., Strader, J., et al. 2023, ApJ, 946, 88
Papitto, A., & de Martino, D. 2022, Astrophys. Space Sci. Lib., 465, 157
Patruno, A., & Watts, A. L. 2021, Astrophys. Space Sci. Lib., 461, 143
Pavlinsky, M. N., Grebenev, S. A., & Sunyaev, R. A. 1994, ApJ, 425, 110
Peng, F., Brown, E. F., & Truran, J. W. 2007, AIP Conf. Ser., 924, 513
Podsiadlowski, P., Han, Z., & Rappaport, S. 2003, MNRAS, 340, 1214
Qiao, E., & Liu, B. F. 2019, MNRAS, 487, 1626
Reig, P., van Straaten, S., & van der Klis, M. 2004, ApJ, 602, 918
Russell, D. M., Fender, R. P., Hynes, R. I., et al. 2006, MNRAS, 371, 1334
Sanna, A., Bahramian, A., Bozzo, E., et al. 2018, A&A, 610, L2
Savonije, G. J., de Kool, M., & van den Heuvel, E. P. J. 1986, A&A, 155, 51
Shaw, A. W., Heinke, C. O., Maccarone, T. J., et al. 2020, MNRAS, 492, 4344
Shaw, A. W., Degenaar, N., Maccarone, T. J., et al. 2024, MNRAS, 527, 7603
Soleri, P., & Fender, R. 2011, MNRAS, 413, 2269
Strohmayer, T., & Bildsten, L. 2006, Camb. Astrophys. Ser., 39, 113

Strohmayer, T. E., Arzoumanian, Z., Bogdanov, S., et al. 2018, ApJ, 858, L13
Tauris, T. M., Langer, N., & Kramer, M. 2012, MNRAS, 425, 1601
Tetarenko, A. J., Bahramian, A., Sivakoff, G. R., et al. 2016, MNRAS, 460, 345
Tetarenko, A. J., Bahramian, A., Wijnands, R., et al. 2018, ApJ, 854, 125
Titarchuk, L. 1994, ApJ, 434, 570
Tudor, V., Miller-Jones, J. C. A., Patruno, A., et al. 2017, MNRAS, 470, 324
van den Eijnden, J., Degenaar, N., Russell, T. D., et al. 2018, Nature, 562, 233
van den Eijnden, J., Degenaar, N., Ludlam, R. M., et al. 2020, MNRAS, 493, 1318
van den Eijnden, J., Degenaar, N., Russell, T. D., et al. 2021, MNRAS, 507, 3899
van den Eijnden, J., Fender, R., Miller-Jones, J. C. A., et al. 2022, MNRAS, 516, 2641
van Haaften, L. M., Nelemans, G., Voss, R., Wood, M. A., & Kuijpers, J. 2012, A&A, 537, A104
van Paradijs, J. 1996, ApJ, 464, L139
van Paradijs, J., & McClintock, J. E. 1994, A&A, 290, 133
Verbunt, F. 1987, ApJ, 312, L23
Verner, D. A., Ferland, G. J., Korista, K. T., & Yakovlev, D. G. 1996, ApJ, 465, 487
Wagg, T., Breivik, K., & de Mink, S. E. 2022, ApJS, 260, 52
White, N. E., Swank, J. H., & Holt, S. S. 1983, ApJ, 270, 711
Wijnands, R., & van der Klis, M. 1998, Nature, 394, 344
Wijnands, R., Degenaar, N., & Page, D. 2017, JApA, 38, 49
Wilson, W. E., Ferris, R. H., Axtens, P., et al. 2011, MNRAS, 416, 832
Wood, K. S., Meekins, J. F., Yentis, D. J., et al. 1984, ApJS, 56, 507